Energy & Buildings 320 (2024) 114607

Contents lists available at ScienceDirect

Energy & Buildings

journal homepage: www.elsevier.com/locate/enb

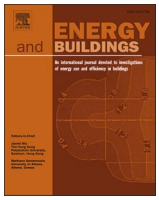

Chance constrained economic dispatch of central air conditionings in large-scale commercial buildings considering demand response

Taoyi Qi, Hongxun Hui *, Yonghua Song

State Key Laboratory of Internet of Things for Smart City, Department of Electrical and Computer Engineering, University of Macau, Macao

ARTICLE INFO

Keywords:
Central air conditioning
Economic dispatch
Chance constraints
Demand response
Commercial buildings

ABSTRACT

Central air conditionings (CACs) deployed in large-scale commercial buildings have consumed a large amount of energy in cities. Growing attention has been expressed in their operating efficiency improvement and demand response (DR) participation to facilitate energy conservation and supply–demand balance. To tackle these challenges, a chance constrained economic dispatch approach is developed for CACs, aimed at optimizing their operation scheduling while accounting for DR participation. Firstly, the economic dispatch framework is established to harness capacity reserves, thermal inertias, and chance constraints to deal with cooling load uncertainties, accompanied by a three-stage DR strategy aimed at augmenting response potential. On this basis, the operation scheduling of CACs is formulated as an optimization problem to minimize overall operating costs considering DR incomes. To solve the problem, the energy-temperature transformation model is developed to quantify available thermal inertias and DR capacities within user comforts. Additionally, chance constraints are converted to specific reserve requirements, to prevent inappropriate dispatches caused by severe but rare forecast errors. Furthermore, the feasible regulation region is designed to coordinate capacity reserves and thermal inertias in response to cooling load forecast errors. Lastly, case studies are conducted using realistic data from commercial buildings, validating the effectiveness of dispatch on operating efficiency improvement, forecast uncertainty accommodation, as well as contributions to DR provision.

1. Introduction

Energy consumed by the building sector contributes to approximately 36 % of global energy demand [1], which is expected to continue increasing with the development of the economy and society [2]. Especially, central air conditionings (CACs) are customarily used in large-scale commercial buildings, e.g., hotel and office buildings, to provide chilled water for space cooling owing to significant cooling capacities, taking up about 50 % of energy proportions within buildings [3]. Meanwhile, the growing penetration of renewable energies in power systems poses challenges to real-time supply–demand balance because of their inherent generation uncertainties [4]. Focusing on the potential supply–demand mismatch risks, Xie and Billinton proposed the unreliability tracing theory to efficiently recognize the critical and weak regions [5]. On this basis, power systems are eager for more flexible regulation capacities in insufficiency regions, which can exactly be provided by CACs due to the large power consumption and thermal inertia [6]. Considering their unique measurement and control advantages over residential air conditionings, it becomes more competitive to realize economic dispatch (ED) and demand response (DR) participation of CACs to facilitate both operating efficiency improvement and renewable energy accommodation.

To promote the sustainable future, a lot of researchers are attracted to investigate new technologies and strategies for CACs with the aim of improving operating efficiency. For instance, Syed et al. [3] presented an adaptive regression model-based strategy to improve the energy efficiency of CACs. Yu et al. [7] proposed a distributed iterative optimization algorithm for chilled water pipe networks, saving energy consumption up to 28.54 %. In terms of large buildings with dramatic cooling demand, central chiller plants with multiple chillers were widely used to satisfy cooling requirements, which are also the major energy-consuming equipment of the CAC systems. Recently, various approaches, such as sequencing control (SC), partial load ratio (PLR) control, and temperature setpoint control, have been utilized to optimize the operation of multi-chiller plants [8]. Among them, SC control is normally implemented in multi-chiller plants to determine the startup and shutdown (SUSD) scheduling of chillers, in response to cooling load fluctuations and PLR variations [9]. In [10], the impacts of multi-chiller

* Corresponding author.
E-mail address: hongxunhui@um.edu.mo (H. Hui).

https://doi.org/10.1016/j.enbuild.2024.114607
Received 22 February 2024; Received in revised form 4 July 2024; Accepted 25 July 2024
Available online 27 July 2024

plant design were evaluated with the aim of further improving energy efficiency on the basis of the SC method. Liao and Huang [11] proposed a hybrid predictive SC strategy, integrating autoregressive with exogenous prediction to double-check the necessity of SC commands, so as to avoid frequent control caused by trivial loads. Unfortunately, the SUSD procedures of chillers are nearly taken into consideration in previous research, like SUSD costs and physical constraints, which may result in lower economic efficiency, worse cooling performance, and even damage to chillers.

Despite the operating efficiency improvement, contributions of large-scale buildings to DR are also repeatedly emphasized in recent years [12], especially in urban cities where flexible regulation resources are extremely insufficient [13]. DR programs are designed to alter or shift energy usage at demand sides to solve short-time power imbalance, preventing investing more regulation resources, e.g., gas turbine generators [14]. Therefore, DR is a promising alternative to enhance the regulation flexibility of power systems [15]. Since buildings play an increasingly important role in the energy sector of urban cities, exploiting their potential in power adjustments is able to effectively cope with fluctuations in both renewable energy generation and load consumption [16]. Benefiting from inherent thermal inertias and building envelopes, the operating power of CACs can be adjusted for a short time without noticeable temperature variations. Much research has been conducted to explore their DR potential. A data-driven approach was investigated to evaluate the operating DR potential in [17], but it focused on residential air conditionings with small capacity and large populations. Xiong et al. developed a simplified improved transactive control strategy to provide DR by adjusting the room set-point temperature [18], while the temperature control made it difficult to realize accurate DR provision. Xie et al. proposed a two-layer coordinated control to aggregate multiple CACs in different buildings to provide regulation services [13], yet the inner coordination of multiple chillers was not accounted for. Besides, the optimization of DR capacity allocation between chillers is also crucial to increase efficiency compared with arbitrary assignments with respect to operating power. Pilot works mainly allocate the regulation or DR capacities based on consensus theory, Hong et al. [19] put forward an event-triggered consensus control to achieve the same regulation objective and response speed of large-scale air conditionings. Li et al. [20] presented a consensus-based energy management for microgrids to guarantee their stability and scalability. Nevertheless, these consensus-based allocation methods aim to achieve equilibrium and unification for different users and equipment, which are not suitable for these chillers within a plant.

Consequently, there are two critical obstacles that need to be overcome before integrating DR participation into the multi-chiller plant optimization, meeting the interests of both power systems and buildings. Firstly, the tradeoff process of ED among thermal comfort, coefficient of performance (COP), and DR performance should be handled appropriately. The load-sharing operation strategy was proposed in [21] to improve the aggregate performance by optimizing the COP of different chillers. However, some potential disadvantages of SUSD are not taken into consideration, e.g., the energy loss caused by the SUSD procedures. In addition, accommodating forecast errors derived from multiple uncertainties is also a challenging problem, many researchers devoted much effort to the improvement of forecast accuracy. A novel energy demand prediction approach was presented in [22] to achieve better prediction accuracy, by combining operating data and empirical knowledge. To some extent, the demand uncertainty can never be mitigated entirely, thereby works with regard to reserve allocation have been investigated recently. For example, Saeedi et al. [23] proposed a robust optimization to deal with the cooling demand uncertainty. However, the robust results are always over-conservative and increase reserve costs. Different from power systems, the cooling process does not need to maintain a strict supply–demand balance, and thermal comforts are not violated with a short period of mismatch. As a result, it is vital to allocate appropriate reserves to accommodate forecast errors, by making the most of the thermal inertia and insulation potential.

Focusing on improving operating efficiency and participating in DR, this paper presents an economic dispatch approach for multi-chiller CACs, coordinately utilizing capacity reserves, thermal inertias, and chance constraints to deal with intrinsic cooling load uncertainties. The main contributions of this paper are as follows:

1) To address the limitations of the conventional methods in managing cooling load fluctuations, specific capacity reserves and DR provisions are determined in the day-ahead operating scheduling to mitigate unnecessary SUSD procedures, accompanied by the three-stage DR strategy aimed at augmenting response potential.
2) Leveraging the insensitivity to slight temperature variations, a temperature-energy transformation (TET) model is developed to quantify thermal inertias within user comforts. Additionally, a feasible regulation region is designed to coordinate capacity reserves and thermal inertias in response to cooling load fluctuations.
3) Chance constraints are further introduced to prevent inappropriate dispatches caused by severe but rare forecast errors. The chance constrained optimization problem is solved by converting the uncertain probability constraints into specific reserve requirements, and then defining that only errors within capacity reserves necessitate complete responses.

The remainder of the paper is organized as follows. Section II introduces the specific ED framework and DR participation strategy of CACs considering forecast uncertainties. The ED of CACs composed of multiple chillers is formulated as an optimization problem in Section III. The developed TET model and the feasible regulation region are presented in Section IV. Section V introduces the simulation results of several case studies. Finally, the main conclusions are summarized in Section VI.

2. ED framework of CACs considering forecast uncertainties and DR participation

Considering the variations and uncertainties of cooling load within a day, ED of CACs aims to achieve the minimum operating costs consisting of operating costs, SUSD costs, and DR income, by determining the SUSD scheduling and optimizing chillers' PLR.

2.1. Framework of economic dispatch for CACs

In terms of large buildings with substantial space cooling demands, multi-type and multi-chiller plants are widely implemented, making full use of the characteristics of different chillers to accommodate complicated operating conditions. To improve the overall energy conversion efficiency, optimizing the SUSD scheduling and corresponding PLR is more important for multi-chiller plants compared to single-chiller CACs. Hence, critical parameters, including the COP-PLR curves and the SUSD costs, should be involved in the total operating costs optimization to allocate cooling capacities among chillers.

As shown in Fig. 1, the forecast cooling load is represented by the blue dot-dash line, and distribution intervals of forecast errors are indicated by the gradient blue area. To cope with the uncertainty of forecast errors and DR participation, the CACs need to reserve appropriate upward and downward capacities to track the varying cooling demand, where the black solid lines are the maximum and minimum cooling capacities under such a chiller scheduling. For deterministic scheduling methods, the forecast errors should be strictly restrained within the regulation regions of chillers to guarantee the cooling demand can be satisfied. Nevertheless, the over-conservative scheduling will lead to a noticeable COP decrease caused by inappropriate operating conditions.

In fact, short-time supply–demand mismatches with preset probabilities (like red star point A) are allowable. Inherent thermal inertias of

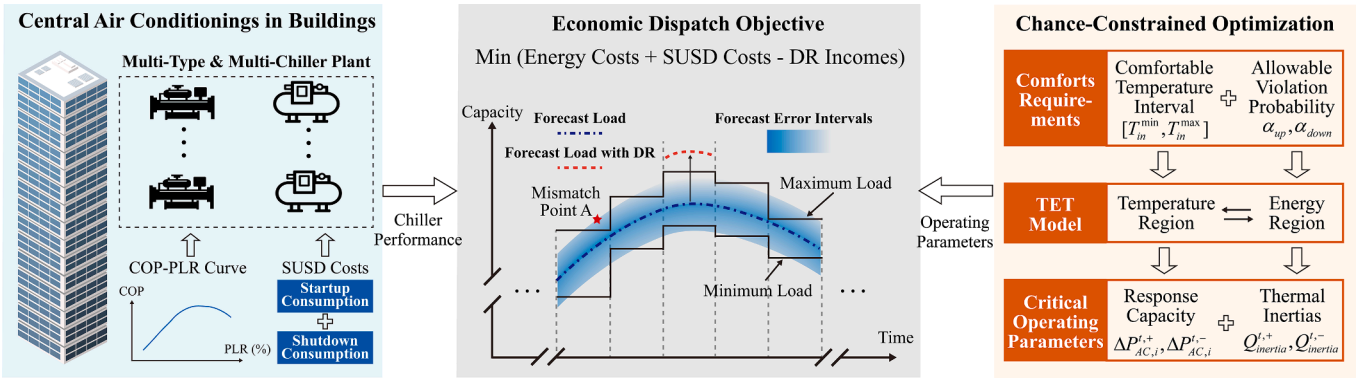

Fig. 1. The framework of economic dispatch for multi-chiller CACs.

buildings can prevent fast temperature variations when there are cooling capacity deviations. To adapt to various thermal comforts, users can choose the preferable indoor temperature intervals and the allowable probability of temperature violations in advance. As a result, the critical challenges are to quantify the thermal inertias derived from temperature intervals and determine the capacity reserves according to violation probabilities. To be specific, the temperature intervals should be transformed into available thermal inertias based on the proposed TET model first. Meanwhile, the upward and downward boundaries of load fluctuations under specific probabilities should be estimated in response to forecast error distribution. Lastly, the critical information including thermal inertias and fluctuation boundaries will be input into the ED optimization model, which will schedule the SUSD procedures and allocate cooling capacities among chillers to mitigate cooling load fluctuations.

2.2. Forecast uncertainty description and thermal comforts requirements

The forecast cooling loads are the basis of ED optimization, there are a lot of methods predicting cooling loads based on historical data. Assuming the forecast cooling load results have been obtained in advance, the cooling load at time t is denoted by D^t_{pred}. Considering forecast errors can never be mitigated entirely, the relationship between forecast values and realistic values D^t_{real} can be expressed as follows [24]:

$$D^t_{real} = D^t_{pred} + \widetilde{e}_t \tag{1}$$

where $\widetilde{e}_t$ is the forecast cooling load error.

Usually, the relevant forecast errors obey the normal distribution whose mean value is equal to zero [25]:

$$\widetilde{e}_t \Big/ D^t_{pred} \sim N(0, \sigma^2) \tag{2}$$

where σ is the variance of the relevant forecast error.

Thermal comforts are the critical criterion to reflect the CAC's performance from the perspective of users. Benefiting from thermal inertias, indoor temperature will not vary dramatically when the cooling supply mismatches the cooling demand. As a result, the intrinsic thermal preservation of buildings delivers the potential energy elasticity: *i*) The SUSD should not be triggered by short-time cooling load variations to avoid extra costs; *ii*) DR capacity can be provided by adjusting operating power within a short period.

In terms of the building with set temperature T^{set}_{in}, to meet the space cooling requirements without sacrificing significant thermal comforts, the real-time indoor temperature T^t_{in} should be constrained within the preset interval:

$$T^{\min}_{in} \leqslant T^t_{in} \leqslant T^{\max}_{in} \tag{3}$$

where $T^{\min}_{in}$ and $T^{\max}_{in}$ represent the minimum and maximum temperatures of the preset interval, respectively.

2.3. Three-stage demand response participation strategy

To mitigate the short-term supply–demand mismatch, DR programs are carried out to extract the power flexibility at the demand side. The multi-chiller plants of CACs contribute to considerable energy consumption in buildings, which can provide substantial DR capacity benefiting from thermal inertia and temperature tolerance. To cope with the time scale of the operation scheduling, CACs participate in day-ahead DR programs, reserving enough time to allocate DR capacities. Let DT_{DR} denote the time duration of DR, two typical DR programs are introduced as follows:

2.3.1. Upward regulation

The CACs should increase the power to consume extra electricity and the indoor temperature will decrease, e.g., at noon when the photovoltaics are harvested.

2.3.2. Downward regulation

The CACs need to decrease the power to reduce the energy consumption and the indoor temperature will increase, e.g., in the afternoon when the energy demands are growing rapidly.

In order to maximize the regulation potential of CACs without affecting the thermal comforts of users, a three-stage DR strategy is proposed in this subsection, namely the pre-regulation stage, the DR-regulation stage, and the post-regulation stage, respectively. The pre-regulation stage and the post-regulation stage aim to expand regulation capacity and restore the initial state, respectively. Usually, the duration time of DR is set as 1 h following the CACs' characteristics and programs' requirements. To prevent fast temperature variations and severe recovery rebounds, the pre-regulation stage and post-regulation are also set as 1 h. Taking the *downward regulation* as an example, the CACs will increase the operating power to realize pre-cooling and store cooling capacity during the pre-regulation stage, accompanied by the corresponding temperature decrease as shown in Fig. 2. Consequently, the available interval of temperature rise is doubled from $\left(T^{\max}_{in} - T^{set}_{in}\right)$ to $\left(T^{\max}_{in} - T^{\min}_{in}\right)$, which can provide extra capacity during the DR-regulation stage by accumulating more heat in rooms. In the post-regulation stage, the operating power is higher than that of the baseline, so as to restore the indoor temperature to the preset value.

Denoting $\Delta P^{t,+(-)}_{AC,i}$ as the DR capacity provided by the i-th chiller at time t, the corresponding power adjustments in pre-regulation and post-regulation can be indicated by $\Delta P^{t-DT_{DR},+(-)}_{AC,i}$ and $\Delta P^{t+DT_{DR},+(-)}_{AC,i}$, respectively. Considering the COP-PLR characteristics, a given DR capacity can never be simply allocated to operating chillers in accordance with their power consumption ratios. Specific optimization of DR allocation will be

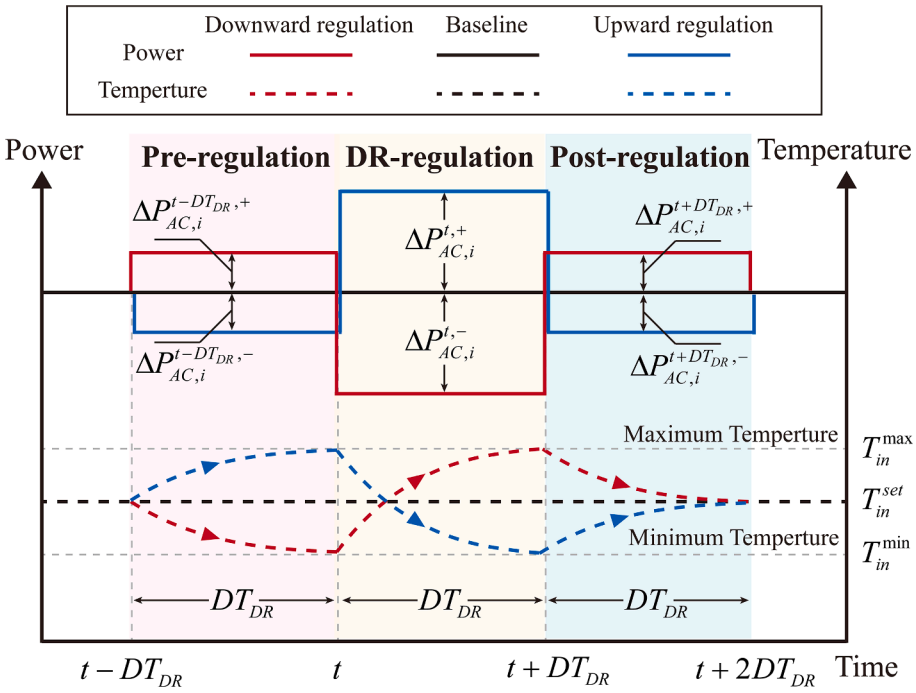

Fig. 2. The specific DR Processes of CACs.

introduced in Section III.

3. Chance constrained economic dispatch problem formulation

The ED of CACs needs to determine the chillers' SUSD scheduling to allocate sufficient reserves in response to uncertain cooling load fluctuations, then further optimize the PLRs of chillers to minimize the overall operating costs with DR participation.

3.1. Objective function

The objective of ED is to determine the optimal SUSD scheduling and allocate cooling loads for multiple chillers, so as to minimize the overall operating costs composed of (*i*) energy costs, (*ii*) SUSD costs, and (*iii*) DR incomes:

$$\min \sum_{t=1}^{t_{end}} \left[\sum_{i=1}^{N_{AC}} \left(EC_i^t + SUSD_i^t \right) - DR^t \right] \tag{4}$$

where t_{end} is the end time of optimization; N_{AC} is the number of chillers.

3.1.1. Energy costs

The energy costs mirror the electricity consumed by chillers to provide chilled water, which mainly depends on the partial load rate (PLR) and their rated power.

$$EC_i^t = PLR_i^t \cdot P_{AC,i}^{rated} \cdot \rho_e^t \tag{5}$$

$$PLR_i^t = P_{AC,i}^t \Big/ P_{AC,i}^{rated} \times 100\% \tag{6}$$

where $P_{AC,i}^t$ and $P_{AC,i}^{rated}$ are the real-time operating power and the rated power of *i*-th chiller, respectively; PLR_i^t is the partial load rate of *i*-th chiller; ρ_e^t is the electricity price per kW.

COP is the critical index to reflect the energy conversion efficiency from electricity to cooling capacity, which is mainly related to the PLR_i^t and can be approximately expressed by the cubic function as follows [11,26]:

$$Q_{AC,i}^t = COP_i^t \cdot P_{AC,i}^t \tag{7}$$

$$COP_i^t = a_i \left(PLR_i^t \right)^3 + b_i \left(PLR_i^t \right)^2 + c_i PLR_i^t + d_i \tag{8}$$

where $Q_{AC,i}^t$ is the real-time cooling load of *i*-th chiller; a_i, b_i, c_i, d_i are the coefficients of the COP-PLR function.

3.1.2. SUSD costs

The SUSD costs are derived from the startup and shutdown procedures, where the chiller is still consuming energy, but little cooling capacity is provided. In the aforementioned works, the SUSD cost is usually ignored. However, inappropriate SUSD scheduling will also lead to substantial costs, especially when there are massive cooling demand oscillations.

$$SUSD_i^t = SU_i^t + SD_i^t \tag{9}$$

$$SU_i^t = \max \left[su_i \left(s_i^t - s_i^{t-1} \right), 0 \right] \tag{10}$$

$$SD_i^t = \max \left[sd_i \left(s_i^{t-1} - s_i^t \right), 0 \right] \tag{11}$$

where SU_i^t and SD_i^t indicate the startup cost and the shutdown cost, respectively; su_i and sd_i are the electricity fees for SUSD processes, respectively; s_i^t is the 0–1 variable that represents the operating state of *i*-th chiller at time *t*.

3.1.3. DR incomes

When providing DR capacity to power systems, the CACs can obtain the corresponding subsidy, whose price per kWh usually is much higher than that of electricity. The total DR incomes depend on the DR capacity and the DR price.

$$DR^t = s_{DR,i}^{t,+} \rho_{DR}^{t,+} \sum_{i=1}^{N_{AC}} \Delta P_{AC,i}^{t,+} + s_{DR,i}^{t,-} \rho_{DR}^{t,-} \sum_{i=1}^{N_{AC}} \Delta P_{AC,i}^{t,-} \tag{12}$$

where $\rho_{DR}^{t,+}$ and $\rho_{DR}^{t,-}$ denote the DR price per kW of *up-regulation* and *down-regulation*, respectively; $\Delta P_{AC,i}^{t,+}$ and $\Delta P_{AC,i}^{t,-}$ represent the power increase and decrease of *i*-th chiller, respectively; $s_{DR,i}^{t,+}$ and $s_{DR,i}^{t,-}$ are 0–1

variables, indicating the states of DR participation.

3.2. Operation constraints

3.2.1. Cooling demand constraints

$$\sum_{i=1}^{N_{AC}} P_{AC,i}^{t} COP_i^t = D_{pred}^{t} \tag{13}$$

where D_{pred}^{t} indicates the forecast total cooling demand at time t. It should be noted that the equation (13) represents the supply–demand balance in the ideal case for the day-ahead schedule. During the real-time operation, the operating power of chillers will be changed with respect to the realistic cooling demand.

3.2.2. Chiller constraints

$$P_{AC,i}^{t} + s_{DR,i}^{t,+} \Delta P_{AC,i}^{t,+} \leqslant s_i^t P_{AC,i}^{\max} \tag{14}$$

$$P_{AC,i}^{t} - s_{DR,i}^{t,-} \Delta P_{AC,i}^{t,-} \geqslant s_i^t P_{AC,i}^{\min} \tag{15}$$

where $P_{AC,i}^{\max}$ and $P_{AC,i}^{\min}$ represent the maximum and minimum operating power of i-th chiller, respectively. Equations (14)-(15) guarantee that the operating power of chillers will not violate the maximum and minimum power constraints during three-stage DR participation.

3.2.3. Minimum on and off time constraints

Considering the physical characteristics of chillers, the SUSD procedures should take some time to finish several default steps, avoiding bad effects such as surges. Besides, reducing unnecessary SUSD procedures can reduce energy consumption, and restrain systems fluctuations [11]. Hence, the chillers must remain *on* or *off* states for preset consecutive time periods after SUSD commands.

$$\sum_{j=t}^{t+DT_{on}-1} s_i^j \geqslant DT_{on}\left(s_i^t - s_i^{t-1}\right), \forall t \in [1, t_{end} - DT_{on} + 1] \tag{16}$$

$$\sum_{j=t}^{t_{end}} \left[s_i^j - \left(s_i^t - s_i^{t-1}\right)\right] \geqslant 0, \forall t \in [t_{end} - DT_{on} + 2, t_{end}] \tag{17}$$

$$\sum_{j=t}^{t+DT_{off}-1} \left(1 - s_i^j\right) \geqslant DT_{off}\left(s_i^{t-1} - s_i^t\right), \forall t \in \left[1, t_{end} - DT_{off} + 1\right] \tag{18}$$

$$\sum_{j=t}^{t_{end}} \left[1 - s_i^j - \left(s_i^{t-1} - s_i^t\right)\right] \geqslant 0, \forall t \in \left[t_{end} - DT_{off} + 2, t_{end}\right] \tag{19}$$

where DT_{on} and DT_{off} are the minimum consecutive time periods after SUSD procedures, respectively.

3.2.4. DR participation constraints

The specific DR capacity and response time periods should be determined and submitted to the operator of power systems. According to the proposed DR participation strategy, the power adjustments of chillers need to satisfy the following requirements.

$$\sum_{i=1}^{N_{AC}} s_{DR,i}^{t,+} \Delta P_{AC,i}^{t,+} - \sum_{i=1}^{N_{AC}} s_{DR,i}^{t,-} \Delta P_{AC,i}^{t,-} = \Delta P_{DR}^{t} \tag{20}$$

$$s_{DR,i}^{t,+} + s_{DR,i}^{t,-} \leqslant 1 \tag{21}$$

where ΔP_{DR}^{t} represents the total DR capacity. The positive value and the negative value mirror the upward regulation and downward regulation, respectively.

Equation (21) limits that only one type of DR capacity can be provided at the same time. However, it is worth noting that different chillers can provide different types of DR regulation at the same time. For clarity, when the multi-chiller plants are delivering upward regulation DR, part of the chillers still can provide downward regulation DR as long as the sum of chillers equals the total DR capacity, which is beneficial for improving the overall operating efficiency. As a result, the specific types and capacities of DR for every chiller also will be optimized in the proposed ED instead of straightforward allocation according to power ratios.

3.2.5. Operating reserve constraints

When the actual cooling load deviates from its forecast value, there should be sufficient upward and downward reserves of cooling capacity to meet the space cooling demands. Different from the conventional PLR-based SC control or robust control, the supply–demand imbalance can be accessible with low probability, since the indoor temperature will not vary notably by utilizing thermal inertia. Consequently, the reserve constraints can be formulated as follows:

$$Pr\left[Q_{inertia}^{t,+} + \sum_{i=1}^{N_{AC}} COP_i^t \left(Res_i^{t,+} - s_{DR,i}^{t,+} \Delta P_{AC,i}^{t,+}\right) \geqslant \widetilde{e}_t\right] \geqslant 1 - \alpha_{up} \tag{22}$$

$$Pr\left[Q_{inertia}^{t,-} + \sum_{i=1}^{N_{AC}} COP_i^t \left(Res_i^{t,-} - s_{DR,i}^{t,-} \Delta P_{AC,i}^{t,-}\right) \geqslant \widetilde{e}_t\right] \geqslant 1 - \alpha_{down} \tag{23}$$

$$Res_i^{t,+} = s_i^t \left(P_{AC,i}^{\max} - P_{AC,i}^{t}\right) \tag{24}$$

$$Res_i^{t,-} = s_i^t \left(P_{AC,i}^{t} - P_{AC,i}^{\min}\right) \tag{25}$$

where $Pr(\cdot)$ represents the probability function; $Q_{inertia}^{t,+}$ and $Q_{inertia}^{t,-}$ are the equivalent upward and downward provided by thermal inertias, respectively; $Res_i^{t,+}$ and $Res_i^{t,-}$ denote the upward and downward reserves, respectively; α_{up} and α_{down} are the maximal allowable probabilities of upward and downward reserve insufficiency, respectively.

4. Economic dispatch procedures

In order to solve the optimization, the TET model is established to quantify the maximum DR capacities and thermal inertias under the given thermal comfort constraints, and chance constraints are converted to specific requirements on capacity reserves according to allowable insufficiency probabilities. Finally, the feasible regulation region is designed to coordinate different resources to accommodate the cooling load uncertainties.

4.1. Temperature energy transformation model

In terms of water-system CACs, the real-time cooling demand satisfied by the multi-chiller plants can be expressed as follows:

$$\sum_{i=1}^{N_{AC}} P_{AC,i}^{t} COP_i^t = m_{sw}^{t} c_w \left(T_{si}^{t} - T_{so}^{t}\right) \tag{26}$$

where m_{sw}^{t} represents the mass flow of water; c_w indicates the specific heat of water; T_{si}^{t} and T_{so}^{t} mirror the inlet and outlet temperature, respectively.

According to equation (26), the cooling capacity depends on the mass flow of water, inlet temperature, and outlet temperature. It is very complicated to analyze the temperature variations when supply cooling capacity mismatches the cooling demand, especially during the DR period. Consequently, the variable water flow control is implemented to guarantee the inlet and outlet temperatures are stable. In other words, the variation of operating power only affects the water flow, and the temperature of chilled water can be regarded as stable at different locations. For the end air handling unit, the supply cooling capacity can be

expressed as follows [27]:

$$Q_{room}^{t} = \lambda_{coe} \cdot m_{wind}^{t} \cdot c_{air} \cdot \left(T_{chill,w}^{t} - T_{in}^{t}\right) \cdot m_{sw}^{t} \tag{27}$$

where Q_{room}^{t} is the cooling capacity for the room; λ_{coe} indicates the wind speed to the infiltration rate; m_{wind}^{t} is the wind speed of the room; c_{air} is the specific heat of air; $T_{chill,w}^{t}$ represents the real-time chilled water temperature at this air handling unit; T_{in}^{t} is the indoor temperature.

Assuming the wind speed m_{wind}^{t} and infiltration rate λ_{coe} are constant and neglecting the minor variations of indoor temperature, the cooling capacity for rooms is regarded as linear with chilled water flow, as well as the total cooling capacity.

$$Q_{room}^{t} \propto m_{sw}^{t} \propto \sum_{i=1}^{N_{AC}} P_{AC,i}^{t} COP_{i}^{t} \tag{28}$$

On this basis, rooms within a building can be regarded as a whole space, because the power regulation has similar effects on cooling capacity in different rooms. Hence, the equivalent thermal parameters model can be used to depict the dynamic process of indoor temperature [28].

$$C_{eq} \frac{\mathrm{d}T_{in}^{t}}{\mathrm{d}t} = \frac{T_{out}^{t} - T_{in}^{t}}{R_{eq}} + Q_{occ}^{t} - D_{pred}^{t} \tag{29}$$

$$D_{pred}^{t} = \sum_{i=1}^{N_{AC}} P_{AC,i}^{t} COP_{i}^{t} \tag{30}$$

where C_{eq} and R_{eq} denote the equivalent thermal capacity and thermal resistance of the building, respectively; T_{out}^{t} represents the ambient temperature, which can be obtained from weather forecast; Q_{occ}^{t} mirrors the other thermal loads derived from people, equipment, solar, etc.; D_{pred}^{t} is the forecast cooling demand based on historical data.

In the day-ahead operation scheduling, the ED mainly concentrates on the stable states at every timestep. If the cooling supply and cooling demand achieve balance, the indoor temperature will be stable at T_{in}^{set}. As a result, the $\mathrm{d}T_{in}^{t}/\mathrm{d}t$ at left-hand is equal to zero, and the other thermal loads Q_{occ}^{t} and the heat exchange Q_{exc}^{t} can be obtained as follows:

$$Q_{occ}^{t} = \sum_{i=1}^{N_{AC}} P_{AC,i}^{t} COP_{i}^{t} - Q_{exc}^{t} \tag{31}$$

$$Q_{exc}^{t} = \frac{T_{out}^{t} - T_{in}^{set}}{R_{eq}} \tag{32}$$

Based on the established TET model, the specific DR capacity can be determined with respect to the allowable temperature intervals. Generally, the DR subsidy per kW is much higher than the electricity price. Hence, buildings always tend to provide more DR capacity within thermal comforts, aiming to minimize the total operation costs. Taking the downward DR as an example, the maximum DR capacity can be obtained by solving the minimum cooling capacity of the chillers according to equations (3) and (29)-(32).

$$\Delta P_{DR}^{t,-} \cdot COP_{avg}^{t} = D_{pred}^{t} - Q_{occ}^{t} - \frac{T_{out}^{t}}{R_{eq}} - \frac{T_{in}^{\min} e^{-\frac{DT_{DR}}{R_{eq}C_{eq}}} - T_{in}^{\max}}{R_{eq}\left(1 - e^{-\frac{DT_{DR}}{R_{eq}C_{eq}}}\right)} \tag{33}$$

$$COP_{avg}^{t} = D_{pred}^{t} \Big/ \sum_{i=1}^{N_{AC}} P_{AC,i}^{t} \tag{34}$$

Similarly, the corresponding power adjustments in the pre-regulation and post-regulation stages can be calculated as follows:

$$\Delta P_{DR}^{t',+} \cdot COP_{avg}^{t'} = D_{pred}^{t'} - Q_{occ}^{t'} - \frac{T_{out}^{t'}}{R_{eq}} - \frac{T_{in}^{set} e^{-\frac{DT_{DR}}{R_{eq}C_{eq}}} - T_{in}^{\min}}{R_{eq}\left(1 - e^{-\frac{DT_{DR}}{R_{eq}C_{eq}}}\right)} \tag{35}$$

$$\Delta P_{DR}^{t'',+} \cdot COP_{avg}^{t''} = D_{pred}^{t''} - Q_{occ}^{t''} - \frac{T_{out}^{t''}}{R_{eq}} - \frac{T_{in}^{set} e^{-\frac{DT_{DR}}{R_{eq}C_{eq}}} - T_{in}^{\min}}{R_{eq}\left(1 - e^{-\frac{DT_{DR}}{R_{eq}C_{eq}}}\right)} \tag{36}$$

$$t' = t - DT_{DR}, t'' = t + DT_{DR} \tag{37}$$

4.2. Reserve determination considering thermal inertias and chance constraints

To guarantee thermal comforts, indoor temperature should be restricted within the preset temperature interval. However, the temperature interval cannot be directly used in the optimization. Hence, quantifying the flexibility of power adjustments is dispensable. Based on the established TET model, the preset temperature interval can be transformed to thermal inertias that can be regarded as equivalent capacity reserves, so as to reduce reserves provided by chillers. Therefore, the upward and downward thermal inertias in equations (22) and (23) can be calculated as follows:

$$Q_{inertia}^{t,+} = D_{pred}^{t} - Q_{occ}^{t} - \frac{T_{out}^{t}}{R_{eq}} - \frac{T_{in}^{set} e^{-\frac{\Delta DT}{R_{eq}C_{eq}}} - T_{in}^{\max}}{R_{eq}\left(1 - e^{\frac{-\Delta DT}{R_{eq}C_{eq}}}\right)} \tag{38}$$

$$Q_{inertia}^{t,-} = D_{pred}^{t} - Q_{occ}^{t} - \frac{T_{out}^{t}}{R_{eq}} - \frac{T_{in}^{set} e^{-\frac{\Delta DT}{R_{eq}C_{eq}}} - T_{in}^{\min}}{R_{eq}\left(1 - e^{\frac{-\Delta DT}{R_{eq}C_{eq}}}\right)} \tag{39}$$

where ΔDT is the timestep of dispatch and optimization.

Furthermore, the specific boundaries with the allowable insufficiency probabilities in equations (22) and (23) should be determined to solve the chance constrained optimization. Assuming the relative forecast errors of cooling load obey the normal distribution, the probability density function of forecast error can be illustrated in Fig. 3 (a). In terms of equation (22), there will be a value K_{α} satisfying the following equation with a determined confidence coefficient α_{up}:

$$Pr\left[K_{\alpha}^{up} \geqslant \tilde{e}_{t}\right] = 1 - \alpha_{up} = \Phi\left(K_{\alpha}^{up}\right) \tag{40}$$

$$\Phi\left(K_{\alpha}^{up}\right) = \int_{-\infty}^{K_{\alpha}^{up}} Pr\left(\tilde{e}_{t}\right) \tag{41}$$

where $\Phi(\cdot)$ is the probability distribution function.

As shown in Fig. 3 (a), $\Phi\left(K_{\alpha}^{up}\right)$ is the integration of the shadow area. Apparently, equation (22) is satisfied if and only if equation (42) is satisfied:

$$Q_{inertia}^{t,+} + \sum_{i=1}^{N_{AC}} COP_{i}^{t}\left(Res_{i}^{t,-} - s_{DR,i}^{t,-} \Delta P_{AC,i}^{t,-}\right) \geqslant K_{\alpha}^{up} \tag{42}$$

To maximize the feasible regulation region, the minimum value that satisfies $K_{\alpha}^{up} = \Phi^{-1}\left(1 - \alpha_{up}\right)$ will be chosen.

$$K_{\alpha}^{up} = \inf\left\{K | K = \Phi^{-1}\left(1 - \alpha_{up}\right)\right\} \tag{43}$$

Similarly, K_{α}^{down} can be determined using the method. Finally, the day-ahead ED problem can be formulated as a mixed integer quadratically constrained programming (MIQCP) problem by transforming the

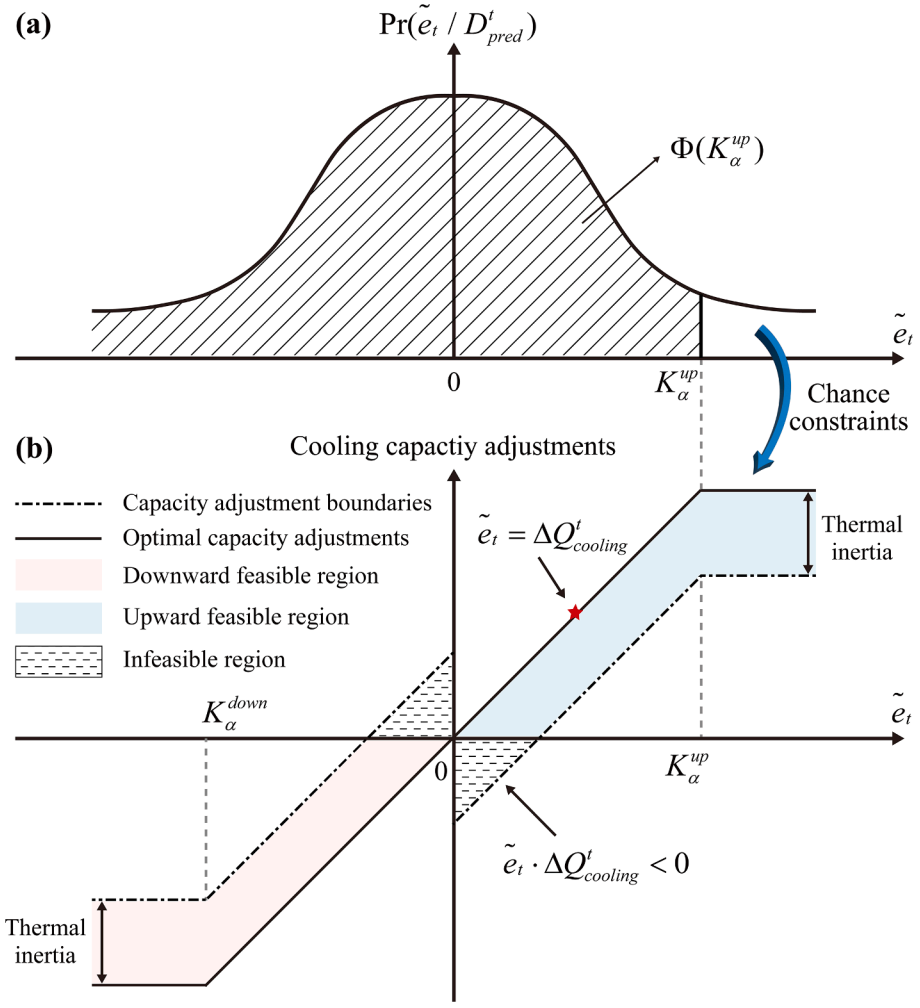

Fig. 3. The feasible regulation region responsible for forecast errors: (a) probability density of forecast errors; (b) response strategy coordinating capacity reserves, thermal inertias, and chance constraints.

COP-PLR curves to piecewise linear expression, which can be solved by various commercial solvers such as GUROBI.

4.3. Intra-day coordinate operation based on feasible regulation region

Although the SUSD scheduling and corresponding PLRs are optimized based on the forecast cooling demand, the forecast errors can never be eliminated. Consequently, CACs also need to further adjust cooling capacity to accommodate forecast errors in intra-day realistic operation. Hence, the feasible regulation region is designed to further dispatch the CACs with the aim of coordinating capacity reserves, thermal inertias, and chance constraints.

Firstly, the SUSD scheduling will not be changed unless extreme weather conditions occur. The specific DR capacity and regulation period are also confirmed in advance. The intra-day optimization objective is to minimize the energy costs at every dispatch timestep:

$$\min \sum_{i=1}^{N_{AC}} EC_i^t, \forall t \in [1, t_{end}] \tag{44}$$

When confronting forecast errors in the intra-day operation, CACs need to adjust cooling capacity to maintain the indoor temperature. In most conventional control approaches, the optimal capacity adjustments should be equal to the forecast errors, which are represented by the black solid line in Fig. 3 (b). In this paper, there are three resources and strategies for eliminating the deviations: *i*) Cooling capacity reserves: the PLRs of chillers can be regulated to realize upward and downward adjustments; *ii*) Thermal inertias: the equivalent reserves derived from thermal inertias can be utilized to reduce adjustments of chillers; *iii*) Allowable insufficiency probability: the supply–demand mismatch is acceptable with the preset probability when there are severe but rare deviations. The coordination of the three resources and strategies is demonstrated in Fig. 3 (b).

The black solid line is the optimal adjustment curve, in which cooling capacity adjustments are equal to the forecast errors like the red star point. Benefiting from thermal inertias, the adjustments are not required to strictly match the errors. When forecast errors are within the interval $\left[K^{down}_\alpha, K^{up}_\alpha\right]$ obtained by allowable insufficiency probabilities, the equivalent reserves derived from thermal inertia can be utilized. The constraints can be expressed as follows:

$$\Delta Q^t_{adj} + Q^t_{inertia} = \tilde{e}_t, K^{down}_\alpha \leqslant \tilde{e}_t \leqslant K^{up}_\alpha \tag{45}$$

where ΔQ^t_{adj} and $Q^t_{inertia}$ are cooling capacity adjustments and reserve capacity derived from thermal inertia, respectively.

It should be noted that thermal inertias are always utilized to reduce the effects caused by forecast errors. To be specific, the positive forecast error means that more cooling capacity is expected to increase to limit the temperature growth, so the downward thermal inertia instead of the upward thermal inertia is used to reduce the capacity adjustment. Similarly, only the upward thermal inertia is utilized when the forecast error is negative. Consequently, the upward and downward thermal

Table 1
Information of the building.

	Floor area	Average height	Thermal resistance	Thermal capacity	Set Temperature	Maximum Temperature	Minimum Temperature
Value	268,000	3.5	4.58×10^{-4}	3.39×10^{2}	24	25	23
Units	m^2	m	℃/kW	kWh/℃	℃	℃	℃

inertias have formulated the regulation boundaries, which are represented by the black dot-dashed lines. Moreover, $Q^t_{inertia}$ is also a decision variable to be optimized. How much thermal inertia is used can be adjusted with the aim of reducing energy costs. To avoid overuse of thermal inertia, the thermal inertia and cooling capacity adjustments need to satisfy:

$$Q^{t,-}_{inertia} \leqslant Q^t_{inertia} \leqslant Q^{t,+}_{inertia} \tag{46}$$

$$\Delta Q^t_{adj} \cdot \widetilde{e}_t \geqslant 0 \tag{47}$$

Equation (47) requires that the cooling capacity adjustments and forecast errors should be positive or negative values at the same time, preventing the situation that the CACs are always likely to reduce the cooling capacity. Consequently, the final adjustments can be chosen within the feasible regions filled with light blue and pink colors in Fig. 3 (b).

Despite the capacity reserves and thermal inertias, chance constraints are further introduced to handle the severe but rare forecast errors. The probability of severe errors is very low, so it is uneconomic to reserve extra capacities to deal with low-possibility events. Therefore, chance constraints are utilized to determine the required reserves under the given insufficiency possibilities. Upon the forecast errors exceed the interval $\left[K^{down}_{\alpha}, K^{up}_{\alpha}\right]$, the supply–demand mismatch is allowable, so the cooling power adjustment will not increase continuously:

$$\begin{cases} \Delta Q^t_{adj} + Q^t_{inertia} = K^{up}_{\alpha} & \widetilde{e}_t \leqslant K^{up}_{\alpha} \\ \Delta Q^t_{adj} + Q^t_{inertia} = K^{down}_{\alpha} & \widetilde{e}_t \leqslant K^{down}_{\alpha} \end{cases} \tag{48}$$

Additionally, chiller constraints (equations (14) and (15)), as well as DR constraints (equations (20) and (21)) should also be satisfied. The intra-day optimization still can be converted to an MIQCP problem.

5. Case study

In this section, simulations on a hotel building with 268,000 m^2 cooling space in Macao, China, are conducted to validate the effectiveness of the proposed chance-constrained ED for efficiency improvement and DR provision.

5.1. Simulation parameters

The information of the building is shown in Table 1. The thermal resistance can be estimated according to the cooling space [29]. The average height of rooms is set as 3.5 m, so the thermal capacity of the building can be obtained according to the volume of cooling space [30]. The temperature setpoint is set to be 24℃, and the allowable temperature interval is set as [23℃, 25℃] considering relatively high thermal comforts requirements [31]. The maximal insufficiency probabilities of upward reserve and downward reserve are set as 10 % uniformly due to the lower requirements on real-time supply–demand balance [32].

The multi-chiller plants of CACs are composed of 2 types of chillers, larger cooling capacity chillers with lower COP and smaller capacity chillers with higher COP, whose specific information is shown in Table 2. The coefficients of COP-PLR curves for two types of chillers are obtained by fitting historical data, and their specific values can be found in Table 2.

The timestep of ED is set as 15 min and there are 96 periods of a day. Referring to the realistic data in the electricity market and ancillary market in Guangdong province, the electricity price and DR subsidy are set as 0.8262¥/kWh and 3.5¥/kWh, respectively. The downward DR will be provided during 14:00–15:00 according to power systems requirements. The following tests have been carried out using Python 3.11.7 and GUROBI 11.0.0 on the desktop with Intel Core i7 12700, the day-ahead operation scheduling and intra-day one-step operation optimization take about 630 s and 0.75 s, respectively.

5.2. Operating costs analysis of different strategies

To illustrate the effectiveness of the proposed ED on operating costs, 4 operating scenarios are set in this subsection: *i*) Scenario 1: the optimal operation at every optimization time step without SUSD costs; *ii*) Scenario 2: the PLR-based SC operation; *iii*) Scenario 3: the PLR-based SC operation with the maximum operation region; *iv*) Scenario 4: the proposed ED operation. Relevant costs and overall operating COPs are shown in Table 3 and Fig. 4, respectively.

Optimal operation strategy aims to determine the optimal chillers commitment and the corresponding PLR to minimize the energy costs at every timestep, so as to provide the important baseline for estimating the effectiveness of the economic dispatch. It should be noted that the SUSD costs and physical constraints are not accounted for. Therefore, the chillers need to start up and shut down very frequently to maintain such a perfect COP, which can be revealed by the SUSD costs calculated afterward. As shown in Table 3, the energy costs are 90,120¥, which can be regarded as the minimum energy costs. The results can be easily explained by the COP profiles in Fig. 4, the COP nearly maintains at the highest value about 6.08 all the time. It can be seen that the actual SUSD costs are 13,016¥ sharing 14.44 % of energy costs, proving that inappropriate SUSD procedures will lead to significant costs. As a consequence, the balance between operating efficiency and SUSD costs is of

Table 3
Operating costs analysis among 3 operating scenarios.

Scenario	Energy costs/¥	Startup costs/¥	Shutdown costs/¥
1	90,120	7,247	5,769
2	93,123	1,510	154
3	94,327	1,295	0
4	90,818	1,478	154

Table 2
Information of multi-type chillers.

	Number	Rated capacity	Rated power	Rated COP	Minimum PLR	Maximum PLR	Coefficient			
							a	b	c	d
Type 1	8	4,220	747	5.65	50	100	–23.59	37.98	–13.25	4
Type 2	4	1,759	295	5.96	50	100	–5.98	6.04	2.93	3
Units	\	kW	kW	\	%	%	\	\	\	\

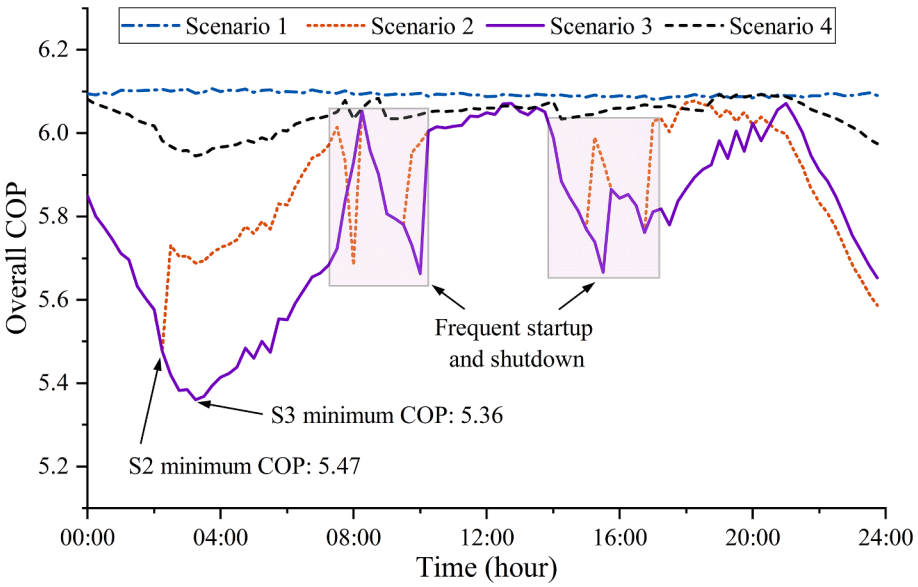

Fig. 4. The variations of COP in different scenarios.

great importance.

The conventional PLR-based SC operation strategy usually determines the SUSD procedures in response to the real-time PLR, which can be realized by automatic or manual processes. When PLR exceeds the upward threshold, e.g., 95 % in this paper, another chiller will be started up to meet the cooling demand. Similarly, once the PLR is below the downward threshold which is set as 70 %, one of the operating chillers will be shut down to increase the overall PLR, avoiding lower operating efficiency. Compared with scenario 1, the PLR-based SC operation spends more energy costs due to the unavoidable operating periods with lower COP. As shown in Fig. 4, the operating COP is always lower than that of scenario 1 caused by the passive startup and shutdown, especially during 00:00–06:00 and 22:00–00:00 periods, whose minimum COP has reached 5.47. On the contrary, the startup and shutdown costs are reduced significantly, which are only 20.84 % and 2.67 % of those in scenario 1, respectively.

To illustrate the potential effects caused by the threshold, the upper threshold and lower threshold of the PLR-based SC operation are changed from 95 % and 70 % to 99 % and 51 % in scenario 3, respectively. It can be seen that the wider PLR region leads to lower operating COP, because chillers will not be shut down even if the PLR is low. For clarity, when the PLR is lower than 70 % and the COP reaches 5.47, partial chillers are shut down to improve the operating COP in scenario 2. On the contrary, chillers will not be shut down in scenario 3, resulting in a minimum COP of 5.36 and a continuous operating period with low COP. Finally, the total energy costs of scenario 3 reach 94,137¥, which increase by 1,204¥ compared to those of scenario 2, while the SUSD costs decrease a little due to fewer startup and shutdown procedures. Consequently, the total operating costs increase by 2.35 %, proving that operating efficiency and reserve sufficiency are contradictory targets when determining the width of the operation region.

In terms of the proposed ED method, the energy costs and SUSD costs are uniformly optimized. As a result, the SUSD procedures are scheduled in accordance with the whole-day operation instead of the real-time PLR. In other words, the SUSD scheduling is more farsighted, so the energy costs are saved effectively. Compared with scenario 2, the COP is

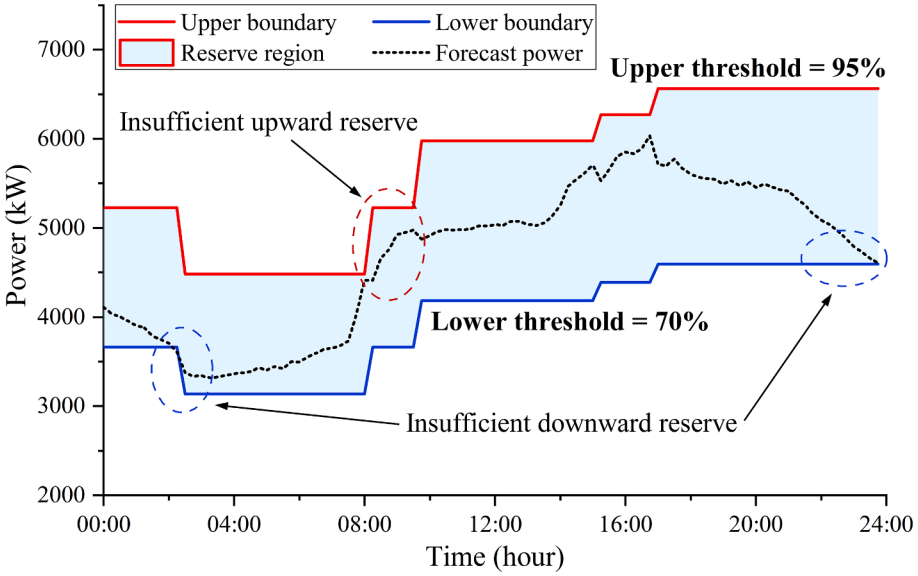

Fig. 5. Reserve analysis of PLR-based SC considering the forecast uncertainty.

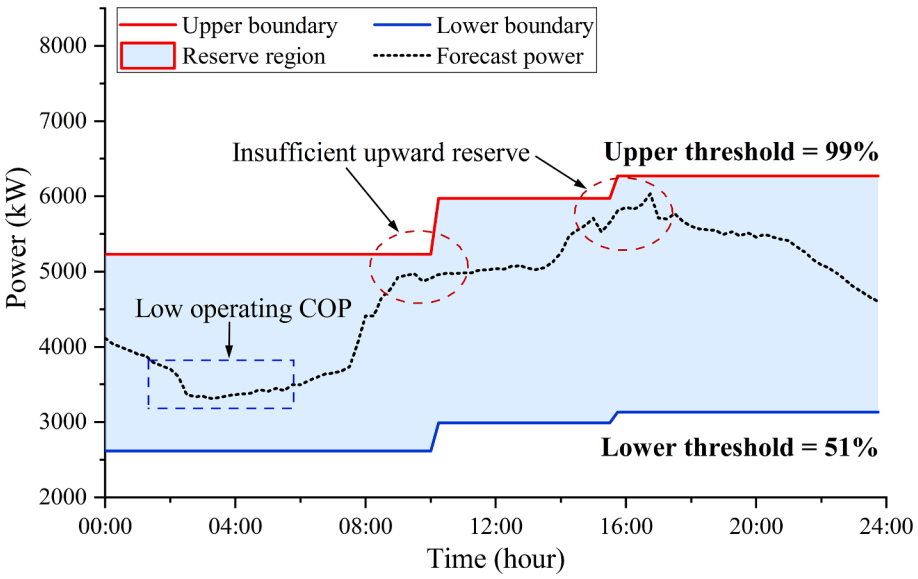

Fig. 6. Reserve analysis of PLR-based SC with a wider operation region considering the forecast uncertainty.

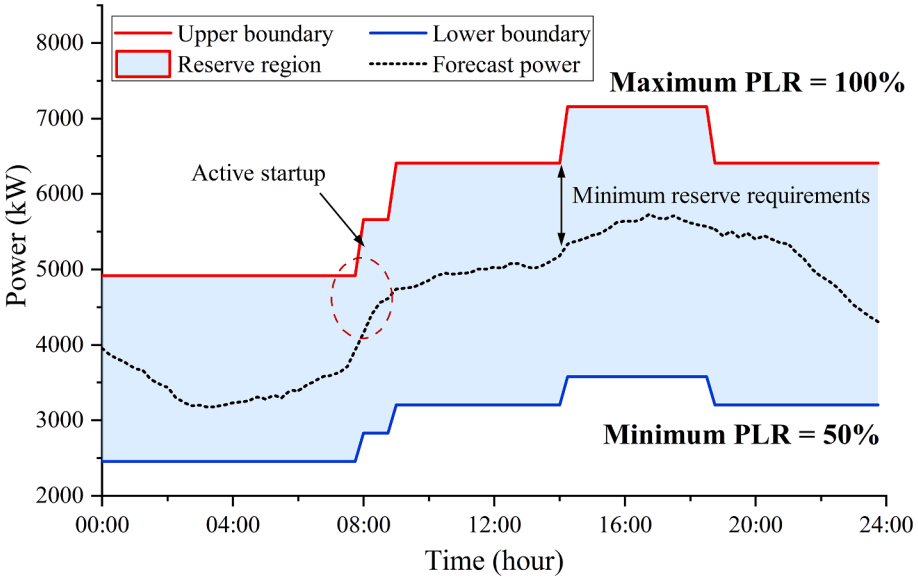

Fig. 7. Reserve analysis of ED considering the forecast uncertainty.

optimized to keep at a much higher level with minor deviations of the optimal COP profiles apart from several periods, thereby the total energy costs saving has reached 2,305¥. Moreover, the unnecessary SUSD procedures are also restrained like those in scenario 2, even startup costs are a little lower. Briefly speaking, the proposed ED method can achieve approximate optimal energy costs without extra SUSD costs.

5.3. Reserve adequacy analysis for day-ahead dispatch

In reality, the forecast errors of cooling demand can never be eliminated due to various uncertain factors such as time-varying population. Consequently, the upward and downward cooling capacities should be reserved to accommodate the cooling demand fluctuations, otherwise the startup or shutdown actions will be taken. Therefore, the differences between the PLR-based SC strategy and the proposed ED method are further analyzed from the perspective of reserve adequacy for load uncertainty in this subsection.

As shown in Fig. 5, the black dotted line indicates the operating power according to forecast cooling demand. The light blue area represents the feasible regulation region of chillers, whose upper boundary and lower boundary are determined by the corresponding SUSD thresholds. It is worth noting that the operating power profiles of the two strategies have some differences, which are caused by the operating COP variations under the same cooling demand. Obviously, the reserve allocation of the PLR-based SC method makes it difficult to trace the variations of cooling demand, because the SUSD operations are always passively taken when the reserves are completely utilized. Therefore, the conditions where reserves are insufficient can never be prevented. For instance, smaller cooling demand fluctuations still lead to insufficient downward reserve at 02:00.

For the conventional PLR-based SC, using a narrower feasible region aims to shut down partial chillers when the PLR is low, so as to avoid lower operating COP. The reserve insufficiency problem is more severe for the PLR-based SC. In terms of scenario 3 as shown in Fig. 6, the upper threshold and lower threshold are changed to 99 % and 51 %, respectively. It can be seen that the insufficient downward reserve problem is solved effectively due to a significant decrease in the lower threshold. However, the upward reserve is still insufficient, since extra chillers are

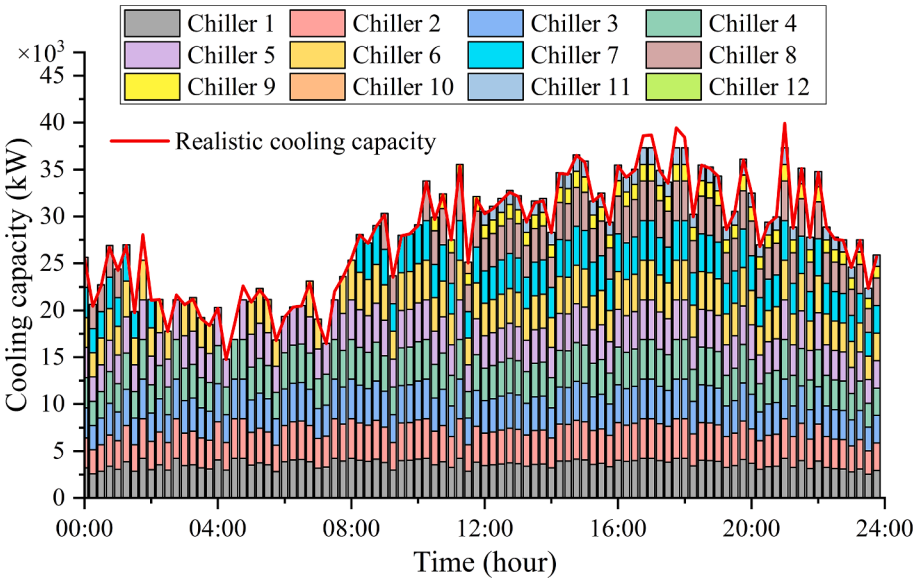

Fig. 8. Realistic operation of the SC method.

started up only when the PLR reaches the upper threshold.

Compared with the PLR-based SC method, the proposed ED method mainly has 2 advantages as nicely shown in Fig. 7. Firstly, the feasible regulation region is expanded dramatically, whose upper boundary and lower boundary are determined by the rated maximum and minimum operating PLRs. To be specific, the lower PLR is also acceptable within a short period to avoid unnecessary SUSD procedures. Then, the SUSD procedures are actively taken with respect to the trends of cooling demand due to the strict reserve constraints. It can be seen that another chiller will be started up once the upward reserves are insufficient at 8:00 and 14:00. Therefore, the upward and downward reserves can better meet uncertainty requirements, so as to prevent unnecessary SUSD procedures and reduce corresponding costs in intra-day realistic operation.

5.4. *Intra-day realistic operation with forecast errors*

Because of the unavoidable uncertainty, the forecast errors can never be eliminated, which puts forward strict requirements for day-ahead dispatch. Adequate reserves not only can satisfy the cooling demand but also can maintain higher operating efficiency. Consequently, the intra-day realistic operations of the SC method and the ED method are further analyzed in this subsection.

The detailed operating profiles of the PLR-based SC strategy are shown in Fig. 8, there are random fluctuations compared with the forecast cooling demand. In terms of the PLR-based SC method, the day-ahead operation results have little guidance for the realistic operation, because its critical parameter is still the PLR. Unfortunately, the frequent cooling demand oscillations have led to similar variations for PLR, the chillers will be started up or shut down continually to trace the short-time demand fluctuations, especially when the PLR is located at the thresholds. Besides, the thermal inertia is not fully utilized so the chillers are always regulated to match the cooling demand as far as possible, further aggravating the operating efficiency. Therefore, both startup and shutdown costs have increased dramatically from 1,510¥ and 154¥ to 2,619¥ and 1,388¥ compared with the day-ahead operation. In addition,

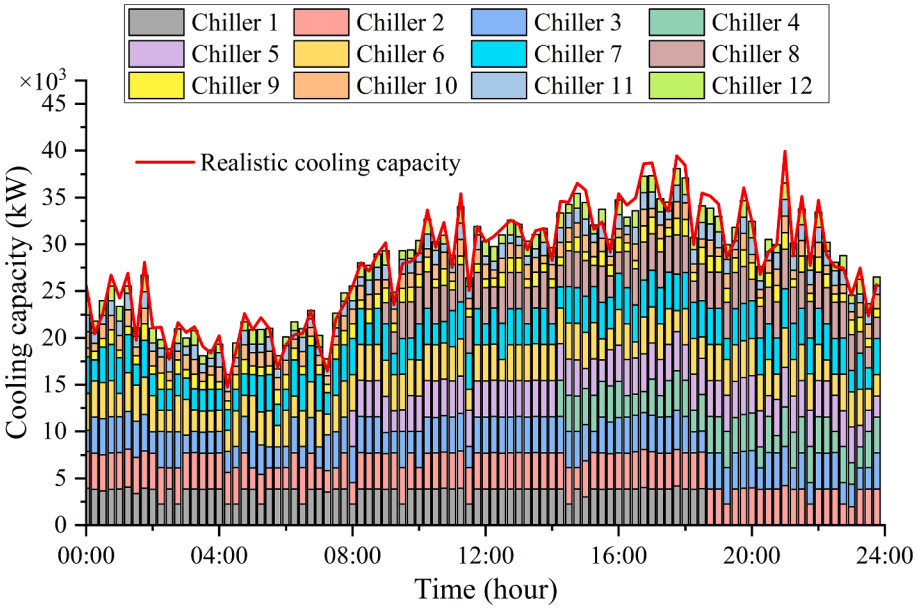

Fig. 9. Realistic operation of the ED method.

Table 4
Realistic operating costs analysis between SC and ED methods.

Method	Energy costs/¥	Startup costs/¥	Shutdown costs/¥
SC	95,606	2,619	1,388
ED	91,689	1,323	0

more SUSD procedures also mean a decrease in efficiency, the energy costs have increased by about 2.57 % to 95,606¥ as shown in Table 4.

On the contrary, the SUSD scheduling of chillers has been determined and adequate cooling capacity has been reserved for the uncertainty by utilizing the proposed ED method. The intra-day operation optimization concentrates on the adjustments of cooling capacity and utilization of thermal inertia as shown in Fig. 9. Hence, there will not be extra SUSD costs unless extreme conditions appear.

Specifically, the proposed ED method has taken full advantage of the thermal inertia and chance constraint without influencing thermal comforts noticeably. The detailed cooling capacity deviations and the corresponding temperature variations are shown in Fig. 10. The light blue and light orange columns represent the extra and missing cooling capacity compared with the cooling demand, respectively. Under most situations, the cooling capacity deviations are restrained within the thermal inertia about 1,350 kW, and the specific utilizing capacity of thermal inertia is also time-varying. Therefore, the indoor temperature can also be maintained in the more comfortable intervals [23.5℃, 24.5℃]. However, there exists a point where the indoor temperature is beyond the upper limit caused by the significant mismatch of cooling capacity. At this moment, the chance constraints have made sense to allow the deviations under the preset probability, otherwise, another chiller needs to be started up just to satisfy such a short period of cooling demand. Benefiting from the thermal inertia and chance constraints, the energy costs of the ED strategy only increase to 91,689¥.

Consequently, the proposed ED strategy has better operating performance under realistic operating conditions, which achieves 6.63 % total cost savings compared with the SC.

5.5. DR contribution to power systems

Based on the intra-day realistic operation results in V.D, the DR participation of CACs is further analyzed to validate the contributions to power systems in this subsection. According to equations (33)-(37), the power adjustments of the pre-regulation period, DR-regulation period, as well as post-regulation period can be obtained, whose values are −180 kW, 360 kW, and −180 kW, respectively.

The detailed capacity allocations of chillers are shown in Fig. 11 during the three-stage DR participation. Instead of simply dividing the power adjustments by the percentage of operating power, the power adjustments of chillers are allocated based on their operating characteristics to achieve overall optimality. For clarity, regulating the operating power of a chiller may improve its efficiency if the latter PLR is nearer the optimal value, so the critical problem is to dispatch chillers coordinately, which is difficult to achieve using the conventional PLR-based SC strategy.

It can be seen from Fig. 11 that there mainly exists three main features: *i*) With respect to the same chiller, the upward and downward DR capacity can never be provided at the same time; *ii*) Some chillers are permitted to provide inverse DR capacity, e.g., chiller 2 with pink color has provided upward capacity while the whole CACs are reducing operating power at 14:45. There always exists both upward and downward power adjustments at the same time, which can improve the overall operating efficiency; *iii*) In terms of the same chiller, the providing DR capacity is also various at different time instants with the same total DR capacity, because the PLR is also optimized in response to the fluctuations of cooling demand.

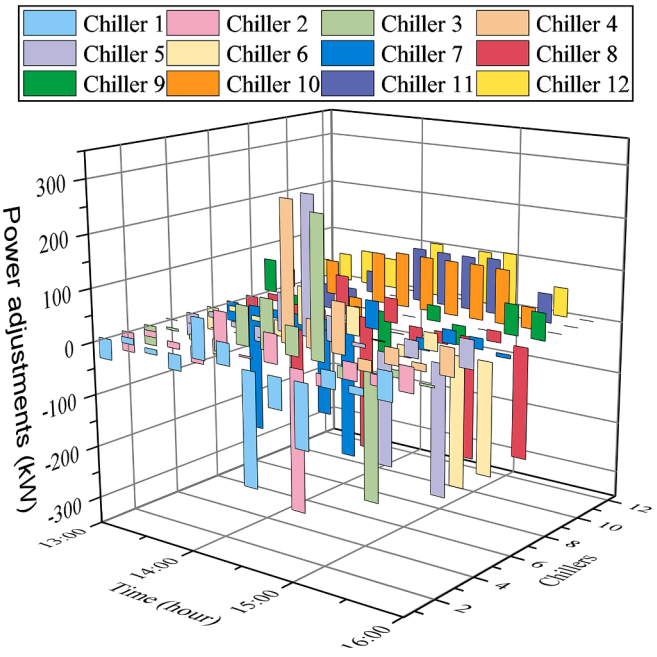

Fig. 11. Specific power adjustments of chillers in DR.

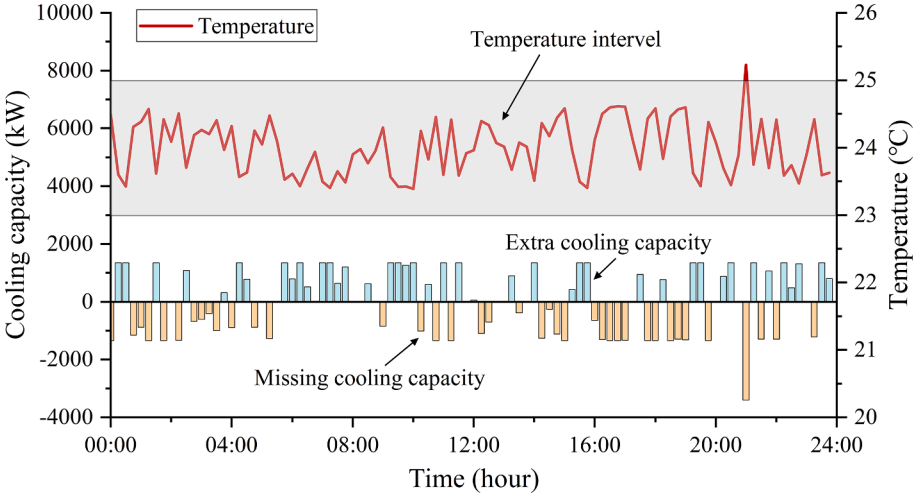

Fig. 10. The cooling capacity deviations and temperature variations.

Finally, the total operating costs are 91,220¥, with 91,157¥ energy costs, 1,323¥ SUSD costs, and 1,260¥ DR income. Generally speaking, the operating costs with DR participation approximately are equal to those without DR, since the consumed energy has little difference by integrating pre-regulation and post-regulation stages. Therefore, the CACs significantly contribute to the flexibility enhancement of power systems without extra energy costs. In addition, the proposed ED method has achieved 8.49 % operating cost savings with DR, compared with the conventional PLR-based SC method.

6. Conclusion

To improve the energy efficiency of CACs and provide DR capacity for power systems, a chance-constrained economic dispatch approach for building CACs is developed to optimize SUSD scheduling and DR participation. By implementing the three-stage DR strategy, the response capacities are effectively expanded within thermal comforts. Then, the day-ahead ED of CACs is formulated as optimization problems to minimize total operating costs considering the COP-PLR features and SUSD constraints, accompanied by an intra-day operation strategy to accommodate cooling load forecast errors by utilizing thermal inertia and chance constraints. Several simulations are conducted, and results prove the effectiveness of the ED method on operating cost saving, operating reserve allocation, as well as significant contributions to DR provision. Finally, the total operating costs have been reduced by 8.49 % compared to the conventional PLR-based SC method.

CRediT authorship contribution statement

Taoyi Qi: Writing – original draft, Validation, Methodology, Formal analysis, Data curation, Conceptualization. **Hongxun Hui:** Writing – review & editing, Visualization, Project administration, Conceptualization. **Yonghua Song:** Supervision, Resources, Investigation, Funding acquisition.

Declaration of competing interest

The authors declare that they have no known competing financial interests or personal relationships that could have appeared to influence the work reported in this paper.

Data availability

The authors do not have permission to share data.

Acknowledgment

The authors are grateful to the China Southern Power Grid Co., Ltd for its support of project SZKJXM20210019. The work is also funded in part by the Science and Technology Development Fund, Macau SAR (File no. 001/2024/SKL, and File no. 0017/2022/A3).

References

[1] Global, A. B. C. 2020 Global Status Report for Buildings and Construction | Globalabc. n.d.
[2] H. Liu, Y. Liu, X. Guo, H. Wu, H. Wang, Y. Liu, An energy consumption prediction method for HVAC systems using energy storage based on time series shifting and deep learning, Energ. Buildings 298 (2023) 113508, https://doi.org/10.1016/j.enbuild.2023.113508.
[3] S.A. Hussain, G. Huang, R.K.K. Yuen, W. Wang, Adaptive regression model-based real-time optimal control of central air-conditioning systems, Appl. Energy 276 (2020) 115427, https://doi.org/10.1016/j.apenergy.2020.115427.
[4] J. Wang, L. Chen, Z. Tan, E. Du, N. Liu, J. Ma, et al., Inherent spatiotemporal uncertainty of renewable power in China, Nat Commun 14 (2023) 5379, https://doi.org/10.1038/s41467-023-40670-7.
[5] K. Xie, R. Billinton, Tracing the unreliability and recognizing the major unreliability contribution of network components, Reliab. Eng. Syst. Saf. 94 (2009) 927–931, https://doi.org/10.1016/j.ress.2008.10.009.
[6] Y. Mu, Y. Xu, J. Zhang, Z. Wu, H. Jia, X. Jin, et al., A data-driven rolling optimization control approach for building energy systems that integrate virtual energy storage systems, Appl. Energy 346 (2023) 121362, https://doi.org/10.1016/j.apenergy.2023.121362.
[7] J. Yu, Q. Liu, A. Zhao, S. Chen, Z. Gao, F. Wang, et al., A distributed optimization algorithm for the dynamic hydraulic balance of chilled water pipe network in air-conditioning system, Energy 223 (2021) 120059, https://doi.org/10.1016/j.energy.2021.120059.
[8] Y. Wang, X. Jin, Z. Du, X. Zhu, Evaluation of operation performance of a multi-chiller system using a data-based chiller model, Energ. Buildings 172 (2018) 1–9, https://doi.org/10.1016/j.enbuild.2018.04.046.
[9] Y. Qi, D. Wang, Y. Lan, H. Jia, C. Wang, K. Liu, et al., A two-level optimal scheduling strategy for central air-conditioners based on metal model with comprehensive state-queueing control models, Energies 10 (2017) 2133, https://doi.org/10.3390/en10122133.
[10] Y. Chen, C. Yang, X. Pan, D. Yan, Design and operation optimization of multi-chiller plants based on energy performance simulation, Energ. Buildings 222 (2020) 110100, https://doi.org/10.1016/j.enbuild.2020.110100.
[11] Y. Liao, G. Huang, A hybrid predictive sequencing control for multi-chiller plant with considerations of indoor environment control, energy conservation and economical operation cost, Sustain. Cities Soc. 49 (2019) 101616, https://doi.org/10.1016/j.scs.2019.101616.
[12] K. Wang, C. Wang, W. Yao, Z. Zhang, C. Liu, X. Dong, et al., Embedding P2P transaction into demand response exchange: A cooperative demand response management framework for IES, Appl. Energy 367 (2024) 123319, https://doi.org/10.1016/j.apenergy.2024.123319.
[13] K. Xie, H. Hui, Y. Ding, Y. Song, C. Ye, W. Zheng, et al., Modeling and control of central air conditionings for providing regulation services for power systems, Appl. Energy 315 (2022) 119035, https://doi.org/10.1016/j.apenergy.2022.119035.
[14] H. Hui, Y. Ding, Q. Shi, F. Li, Y. Song, J. Yan, 5G network-based Internet of Things for demand response in smart grid: A survey on application potential, Appl. Energy 257 (2020) 113972, https://doi.org/10.1016/j.apenergy.2019.113972.
[15] T. Qi, C. Ye, Y. Zhao, L. Li, Y. Ding, Deep reinforcement learning based charging scheduling for household electric vehicles in active distribution network, J. Mod Power Syst. Clean Energy 11 (2023) 1890–1901, https://doi.org/10.35833/MPCE.2022.000456.
[16] Z. Zhang, C. Wang, Q. Wu, X. Dong, Optimal dispatch for cross-regional integrated energy system with renewable energy uncertainties: A unified spatial-temporal cooperative framework, Energy (2024) 130433, https://doi.org/10.1016/j.energy.2024.130433.
[17] N. Qi, L. Cheng, H. Xu, K. Wu, X. Li, Y. Wang, et al., Smart meter data-driven evaluation of operational demand response potential of residential air conditioning loads, Appl. Energy 279 (2020) 115708, https://doi.org/10.1016/j.apenergy.2020.115708.
[18] C. Xiong, Z. Sun, Q. Meng, Z. Li, Y. Wei, F. Zhao, et al., A simplified improved transactive control of air-conditioning demand response for determining room set-point temperature: Experimental studies, Appl. Energy 323 (2022) 119521, https://doi.org/10.1016/j.apenergy.2022.119521.
[19] J. Hong, H. Hui, H. Zhang, N. Dai, Y. Song, Event-triggered consensus control of large-scale inverter air conditioners for demand response, IEEE Trans. Power Syst. 37 (2022) 4954–4957, https://doi.org/10.1109/TPWRS.2022.3204215.
[20] Consensus-Based Energy Management of Microgrid With Random Packet Drops | IEEE Journals & Magazine | IEEE Xplore n.d. https://ieeexplore.ieee.org/document/10035520 (accessed January 25, 2024).
[21] H.Z. Abou-Ziyan, A.F. Alajmi, Effect of load-sharing operation strategy on the aggregate performance of existed multiple-chiller systems, Appl. Energy 135 (2014) 329–338, https://doi.org/10.1016/j.apenergy.2014.06.065.
[22] Z. Chen, Q. Deng, H. Ren, Z. Zhao, T. Peng, C. Yang, et al., A new energy consumption prediction method for chillers based on GraphSAGE by combining empirical knowledge and operating data, Appl. Energy 310 (2022) 118410, https://doi.org/10.1016/j.apenergy.2021.118410.
[23] M. Saeedi, M. Moradi, M. Hosseini, A. Emamifar, N. Ghadimi, Robust optimization based optimal chiller loading under cooling demand uncertainty, Appl. Therm. Eng. 148 (2019) 1081–1091, https://doi.org/10.1016/j.applthermaleng.2018.11.122.
[24] Q. Shi, F. Li, H. Cui, Analytical method to aggregate multi-machine SFR model with applications in power system dynamic studies, IEEE Trans. Power Syst. 33 (2018) 6355–6367, https://doi.org/10.1109/TPWRS.2018.2824823.
[25] L. Liu, D. Xu, C.-S. Lam, Two-layer management of HVAC-based Multi-energy buildings under proactive demand response of Fast/Slow-charging EVs, Energ. Conver. Manage. 289 (2023) 117208, https://doi.org/10.1016/j.enconman.2023.117208.
[26] Z. Liu, H. Tan, D. Luo, G. Yu, J. Li, Z. Li, Optimal chiller sequencing control in an office building considering the variation of chiller maximum cooling capacity, Energ. Buildings 140 (2017) 430–442, https://doi.org/10.1016/j.enbuild.2017.01.082.
[27] B. Cui, C. Fan, J. Munk, N. Mao, F. Xiao, J. Dong, et al., A hybrid building thermal modeling approach for predicting temperatures in typical, detached, two-story houses, Appl. Energy 236 (2019) 101–116, https://doi.org/10.1016/j.apenergy.2018.11.077.
[28] H. Hui, Y. Ding, W. Liu, Y. Lin, Y. Song, Operating reserve evaluation of aggregated air conditioners, Appl. Energy 196 (2017) 218–228, https://doi.org/10.1016/j.apenergy.2016.12.004.
[29] D.S. Callaway, Tapping the energy storage potential in electric loads to deliver load following and regulation, with application to wind energy, Energ. Conver. Manage. 50 (2009) 1389–1400, https://doi.org/10.1016/j.enconman.2008.12.012.

[30] W. Cui, Y. Ding, H. Hui, Z. Lin, P. Du, Y. Song, et al., Evaluation and sequential dispatch of operating reserve provided by air conditioners considering lead-lag rebound effect, IEEE Trans. Power Syst. 33 (2018) 6935–6950, https://doi.org/10.1109/TPWRS.2018.2846270.

[31] H. Hui, Y. Ding, T. Chen, S. Rahman, Y. Song, Dynamic and stability analysis of the power system with the control loop of inverter air conditioners, IEEE Trans. Ind. Electron. 68 (2021) 2725–2736, https://doi.org/10.1109/TIE.2020.2975465.

[32] Y. Yang, W. Wu, B. Wang, M. Li, Analytical reformulation for Stochastic unit commitment considering wind power uncertainty with gaussian mixture model, IEEE Trans. Power Syst. 35 (2020) 2769–2782, https://doi.org/10.1109/TPWRS.2019.2960389.